PROCEEDINGS OF SCIENCE

Rare B decays at CMS including B di-muonic decays.

Paolo Ronchese*
INFN and University of Padova
E-mail: paolo.ronchese@pd.infn.it

The rare decays $B_s(B^0) \to \mu^+\mu^-$ are an excellent test of the flavor sector of the Standard Model and provide sensitivity to models with extended Higgs boson sectors. We report on searches for these decays with the CMS experiment using pp collisions at a centre-of-mass energy $\sqrt{s} = 7$ TeV collected in 2011. In both decays, the number of events observed after all selection requirements is consistent with the expectation from background plus standard model signal predictions. The resulting upper limits on the branching fractions are $\mathfrak{B}(B_s^0 \to \mu^+\mu^-) < 7.7 \times 10^{-9}$ and $\mathfrak{B}(B_d^0 \to \mu^+\mu^-) < 1.8 \times 10^{-9}$ at 95% confidence level.

The XIth International Conference on Heavy Quarks and Leptons
11-15 June, 2012
Prague,The Czech Republic

*Speaker.

PoS(HQL 2012)027

1. Introduction

The decays $B^0_{d,s} \to \mu^+\mu^-$ are highly suppressed in the Standard Model of particles physics. This suppression is due to the flavor-changing neutral current transitions, which are forbidden at tree level and can only proceed via high-order diagrams that are described by electroweak penguin and box diagrams, as shown in fig.1. Additionally, the decays are helicity suppressed by a factor $\left(m_\mu/m_B\right)^2$. Furthermore, these decays require an internal quark annihilation within the B meson that reduces the decay rate by an additional factor $(f_B/m_B)^2$, where f_B is the decay constant of the B meson. As a consequence, the branching ratio are predicted [1] to be $\mathfrak{B}(B^0_s \to \mu^+\mu^-) = (3.2 \pm 0.2) \times 10^{-9}$ and $\mathfrak{B}(B^0_d \to \mu^+\mu^-) = (1.0 \pm 0.1) \times 10^{-10}$.

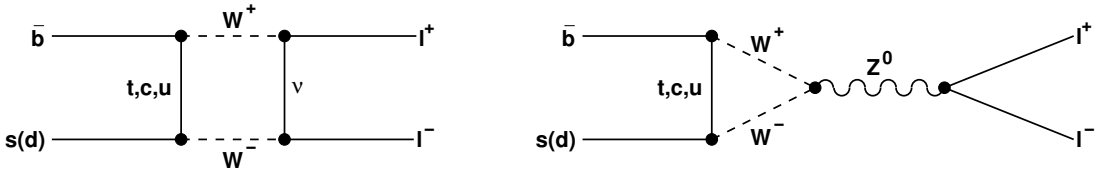

Figure 1: Graphs describing the decays $B^0_{d,s} \to \ell^+\ell^-$ in the standard model.

In Standard Model extensions new particles (e.g., charginos, neutralinos, Higgs bosons, squarks and sleptons) can contribute to the process and thereby can increase the expected branching fraction by orders of magnitude; the ratio R of the branching ratios of B^0_d and B^0_s could also be enhanced [2–7].

A simultaneous search for $B^0_d \to \mu^+\mu^-$ and $B^0_s \to \mu^+\mu^-$ decays using data collected in 2011 by the CMS experiment in pp collisions at $\sqrt{s} = 7$ TeV at the LHC is shown in the following. The dataset corresponds to an integrated luminosity $\mathscr{L} = 5$ fb^{-1}. An event-counting experiment is performed in dimuon mass regions around the B^0_d and B^0_s.

The CMS detector [8] is a general-purpose detector designed and built to study physics at the TeV scale. For this analysis, the main subdetectors used are a silicon tracker, composed of pixel and strip detectors within a 3.8 T axial magnetic field, and a muon detector, which is divided into a barrel section and two endcaps, consisting of gas-ionization detectors embedded in the steel return yoke of the solenoid.

The dimuon candidate events are selected with a two-level trigger system: the first level only uses the muon detector information, while the high-level trigger (HLT) uses additional information from the silicon tracker. Tracks found in the two subdetectors are combined to reconstruct muon candidates. The reconstruction of $B^0_{d,s} \to \mu^+\mu^-$ candidates requires two oppositely-charged muons that originate from a common vertex: a fit of the B-candidate vertex is performed and the two daughter muon tracks are combined to form the B-candidate track.

Monte Carlo simulations are used to estimate backgrounds due to B decays. Combinatorial backgrounds are evaluated from the data in dimuon invariant mass $M_{\mu^+\mu^-}$ sidebands.

The dimuon yield is compared with a "normalization" sample of events with $B^+ \to J/\psi K^+$ decays, followed by the decay $J/\psi \to \mu^+\mu^-$. This procedure allows a cancellation of the uncertainties on luminosity and $b\bar{b}$ production rate, and at least a partial cancellation of the uncertainties

on acceptance and efficiency. The branching ratio $\mathfrak{B}(B_s^0 \to J/\psi\phi \to \mu^+\mu^- K^+K^-)$ is computed in parallel to validate the procedure.

In the CMS detector, the mass resolution, which influences the separation between $B_d^0 \to \mu^+\mu^-$ and $B_s^0 \to \mu^+\mu^-$ decays, depends on the pseudorapidity η of the reconstructed particles. The background level also depends significantly on the pseudorapidity of the B candidate. Therefore, the analysis is performed separately in two channels, "barrel" and "endcap", and then combined for the final result. The barrel channel contains the candidates where both muons have $|\eta| < 1.4$ and the endcap channel contains those where at least one muon has $|\eta| > 1.4$.

2. Data selection and analysis

The normalization procedure gives the branching ratio of $B_{d,s}^0$ to $\mu^+\mu^-$ from the ratio of background-subtracted events in the signal sample and the normalization sample, multiplied by the ratio of the corresponding efficiencies of trigger and reconstruction, as shown in eq.2.1.

$$\mathfrak{B}(B_{d,s}^0 \to \mu^+\mu^-) = \frac{N_{\rm sig}}{N_{\rm nrm}} \frac{\varepsilon_{\rm nrm}}{\varepsilon_{\rm sig}} \frac{f_u}{f_{d,s}} \mathfrak{B}(B^+ \to J/\psi K^+ \to \mu^+\mu^- K^+) \tag{2.1}$$

An additional factor $f_u/f_{d,s}$ is applied to account for the ratio of production rate of B^+ and B_d^0 or B_s^0. The ratio f_u/f_d is taken as one, while the ratio f_u/f_s is taken from the fraction measured by LHCb [9] $f_s/f_u = 0.267 \pm 0.021$ for $2 < |\eta| < 5$. The branching ratio $\mathfrak{B}(B^+ \to J/\psi K^+ \to \mu^+\mu^- K^+)$ is taken from the world average [11]: $(6.0 \pm 0.2) \times 10^{-5}$.

The search is performed through a blind analysis, so that the signal region with an invariant mass of the dimuon system in the range 5.20 GeV $< M_{\mu^+\mu^-} <$ 5.45 GeV can be inspected only after having defined the selection cuts, measured the trigger and selection efficiencies, estimated the background and the systematic uncertaintes.

2.1 Trigger and muon identification

The first-level trigger requires two muon candidates without any explicit p_T requirement; very low p_T muons are implicitly rejected since they do not reach the muon detectors. At high level a set of cuts are applied; due to the increase of luminosity of LHC during the data taking those cuts have been tightened up to the values listed in the following.

For the signal two muons are required with $p_{T-\mu} > 4$ GeV, a dimuon transverse momentum $p_{T-\mu^+\mu^-} > 3.9$ GeV in the barrel and $p_{T-\mu^+\mu^-} > 5.9$ GeV in the endcap, pseudorapidity $|\eta| < 2.2$, invariant mass in the range 4.8 GeV $< M_{\mu^+\mu^-} <$ 6.0 GeV and a $3D$ distance of closest approach to each other $d_{\rm ca} < 0.5$ cm.

For the normalization two muons are required with $p_{T-\mu} > 4$ GeV, a dimuon transverse momentum $p_{T-\mu^+\mu^-} > 6.9$ GeV, pseudorapidity $|\eta| < 2.2$, invariant mass in the range 2.9 GeV $< M_{\mu^+\mu^-} <$ 3.3 GeV, $d_{\rm ca} < 0.5$ cm, the probability of the χ^2 per degree of freedom of the dimuon vertex fit $\Pi(\chi^2_{\mu^+\mu^-{\rm vertex}}) > 15\%$. Two additional requirements are imposed in the transverse plane: $\cos\alpha_{xy} > 0.9$, where α_{xy} is the pointing angle between the dimuon momentum and the vector from the average interaction point to the dimuon vertex, and $\ell_{xy}/\sigma(\ell_{xy}) > 3$ where ℓ_{xy} is the two-dimensional distance between the primary and dimuon vertices and $\sigma(\ell_{xy})$ is its uncertainty.

Muons are identified by reconstructing and matching track segments in the tracker and the muon detector. It's required having a reconstructed segment in 2 muon detector stations at least, out of 4 present in the whole muon system. It's also required having at least 10 hits in the tracking sytem, and at least one of them is required to be in the pixel detector. A χ^2/d.o.f. < 10 cut on the chisquare per degree of freedom of the combined track is applied and the impact parameter is required to be $d_{xy} < 0.2$ cm.

The trigger and identification efficiencies, both for signal and normalization, are estimated by using the simulation; a measurement based on a "tag and probe" technique [10], applied to $J/\psi \to \mu^+\mu^-$ decays, is performed also in data. A "tag" muon, satisfying strict muon criteria, is paired with a "probe" track, where together they combine to give the J/ψ invariant mass, so that the probe can be assumed to be a muon; the sample of probe tracks can then be used to compute efficiencies. The difference of the results obtained with the "tag and probe" technique in data and simulation is included in the systematic uncertainty. For the signal events the muon identification efficiencys is 71% in the barrel and 85% in the endcap; for the normalization and control samples, the muon identification efficiency is 77% in the barrel and 78% in the endcap.

2.2 Vertices analysis

Opposite charged muons are fitted to a common vertex and combined to form a B meson candidate. Due to the high luminosity of LHC the average number of proton-proton interactions throughout the 2011 data taking was $\bar{N}_{\text{int}} = 8$; to remove the effect of the pileup the primary vertex is chosen as the nearest to the B vertex along the beams direction.

To select a sample of clean candidates of B mesons decaying to a pair of muons, the candidate itself is required to be isolated from the other particles produced in the event. An isolation variable I is built with the ratio

$$I = \frac{p_T(B)}{p_T(B) + \Sigma_{\text{trk}} p_T} \tag{2.2}$$

of the B candidate transverse momentum and the sum of the transverse momenta of all the particles, consistent with coming from the B or the primary vertex, contained in a $\Delta R = \sqrt{(\Delta\phi)^2 + (\Delta\eta)^2} < 0.7$ cone and having $p_T > 0.9$ GeV. Two other variables are used to select isolated candidates: the number N_{close} of tracks with $p_T > 0.5$ GeV and a distance of closest approach to B vertex $d_{\text{ca}} < 0.03$ cm and the minimum distance to B vertex d^0_{ca} for all the tracks. The distribution for the three variables I, N_{close} and d^0_{ca} are shown in fig.2. For each distribution, the selection requirements for all variables, apart from the one plotted, are applied.

The final selection is summarized in table 1 with the cuts on the isolation variables as well as the muon and dimuon p_T, the $3D$ impact parameter and significance, the pointing angle, the vertex chisquare per degree of freedom and the flying distance significance. The total efficiency of the selection is $(0.29 \pm 0.2)\%$ in the barrel and $(0.16 \pm 0.2)\%$ in the endcap.

For normalization and control samples, $B^+ \to J/\psi K^+ \to \mu^+\mu^- K^+$ and $B^0_s \to J/\psi\phi \to \mu^+\mu^- K^+ K^-$, a similar but not identical selection is used; candidates with two oppositely-charged muons sharing a common vertex and with invariant mass in the range 3.0 GeV $< M_{\mu^+\mu^-} <$ 3.2 GeV are reconstructed and combined with one or two tracks assumed to be kaons. Dimuon transverse momentum is required to be $p_T > 7$ GeV and kaons are required to have $p_T >$ 0.5 GeV and $|\eta| < 2.4$; B candidates with an invariant mass in the range 4.8 GeV $< M_B <$ 6.0 GeV

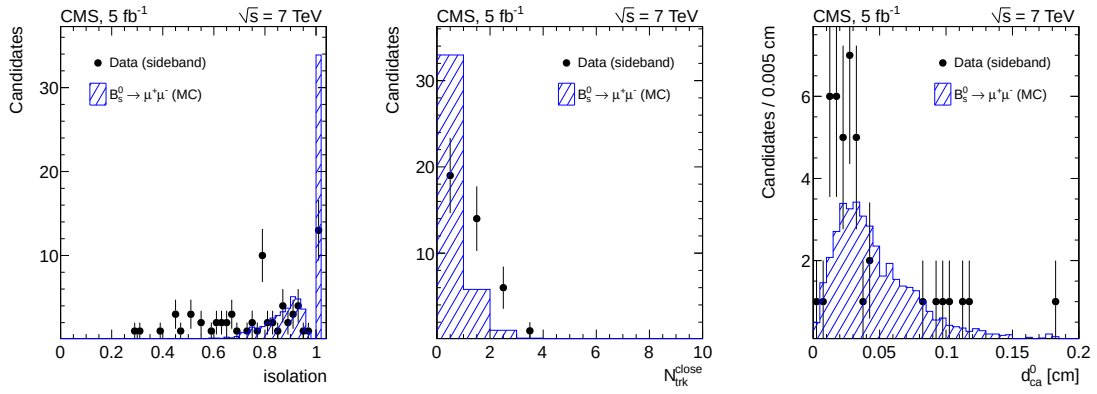

Figure 2: Distribution of the isolation variable I (left), number of close tracks N_{close} (center) and minimum closest approach distance d^0_{ca} (right). The dashed histograms show the distribution in a simulated signal sample while the dots show the distributions for data in sidebands.

variable		barrel	endcap	unit
$p_{\text{T}\mu 1}$	$>$	4.5	4.5	GeV
$p_{\text{T}\mu 2}$	$>$	4.0	4.2	GeV
$p_{\text{T}\mu\mu}$	$>$	6.5	8.5	GeV
δ_{3D}	$<$	0.008	0.008	cm
$\delta_{\text{3D}}/\sigma(\delta_{\text{3D}})$	$<$	2	2	
α	$<$	0.05	0.03	rad
$\chi^2/\text{d.o.f.}$	$<$	2.2	1.8	
$\ell_{\text{3D}}/\sigma(\ell_{\text{3D}})$	$>$	13	15	
I	$>$	0.8	0.8	
d_{ca}	$>$	0.015	0.015	cm
N_{close}	$<$	2	2	

Table 1: Selection criteria for $B^0_s \to \mu^+\mu^-$ and $B^0_d \to \mu^+\mu^-$ search in the barrel and endcap.

are selected. All the tracks coming from the B decay are used in the vertex fit and candidates with $\chi^2/\text{d.o.f.} < 2$ are considered; the $3D$ distance of closest approach between all pairs is required to be $d_{\text{ca}} < 0.1$ cm. For $B^0_s \to J/\psi\phi \to \mu^+\mu^- K^+K^-$ candidates the two kaons are required to have an invariant mass in the range $0.995\ \text{GeV} < M_{KK} < 1.045\ \text{GeV}$ and $\Delta R(K^+K^-) < 0.25$. The total efficiency of the selection for the normalization sample is $(11.0 \pm 0.9) \times 10^{-4}$ in the barrel and $(3.2 \pm 0.4) \times 10^{-4}$ in the endcap, including the detector acceptance and the track finding efficiency.

2.3 Normalization

The invariant mass distributions in the normalization sample are fit with a double-Gaussian function for the signal and an exponential plus an error function for the background, as shown in fig.3. The background shape is chosen to model the effect of partly reconstructed decays, as, for instance, $B^{\pm} \to J/\psi K^*$ where a decay product of the K^* gets lost in the reconstruction. The

number of normalization events is $(82.7 \pm 4.2) \times 10^3$ in the barrel sample and $(23.8 \pm 1.2) \times 10^3$ in the endcap.

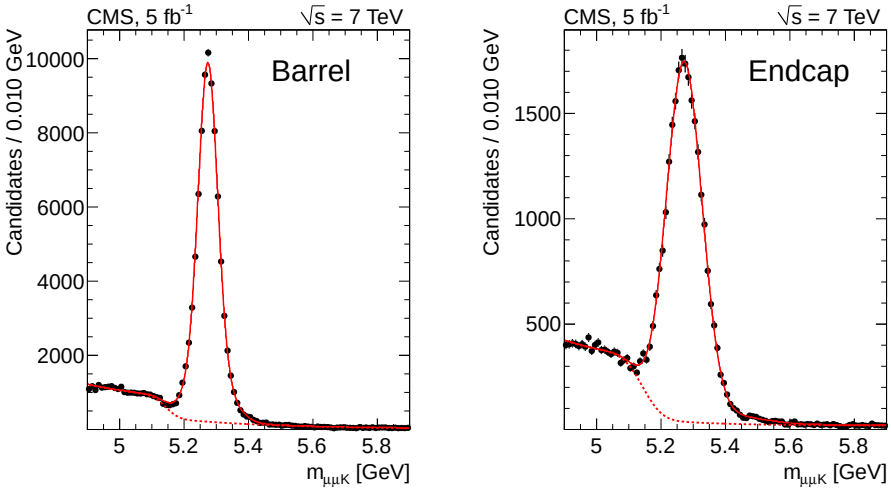

Figure 3: $B^+ \to J/\psi K^+ \to \mu^+\mu^- K^+$ invariant-mass distributions in the barrel (left) and endcap (right) channels. The solid and dashed lines show the fits to the data and background respectively.

2.4 Background

The background in the $B^0_{d,s} \to \mu^+\mu^-$ candidates sample is expected to come from two main sources: one is of physical nature and consists in the decay of B hadrons to a pair of hadrons misidentified as muons ("peaking background") or one muon and an hadron, again misidentifed as a muon (semileptonic decays); the other source is a simple combinatorial background.

The first contribution is estimated from the simulation and applying the misidentification probabilities; they are measured in samples of D^0 decays for kaons and pions and Λ^0 decays for protons: $\Pi_{(\pi,K)\to\mu} = (0.10 \pm 0.02)\%$, $\Pi_{p\to\mu} = (0.05 \pm 0.01)\%$. The expected invariant mass distributions of the background coming from B decays is shown in fig.4.

The combinatorial background is assumed having a flat shape and it is estimated from the data by interpolating into the signal window the number of events observed in sidebands, after subtracting the expected semileptonic background.

3. Systematic uncertainties

Systematic errors can be divided in two classes, one for the sources related to physics and the other for the sources of errors with experimental nature. The systematic errors for all the sources are summarized in table 5.

In the first class there's the acceptance uncertainty associated with the different $b\bar{b}$ production mechanisms, the ratio of B^+ and B^0_s production rates and the misidentified B decays.

Production of $b\bar{b}$ pairs can go through different mechanisms: gluon gluon fusion, flavor excitation and gluon splitting. They have different angular and p_T correlation and as a consequence

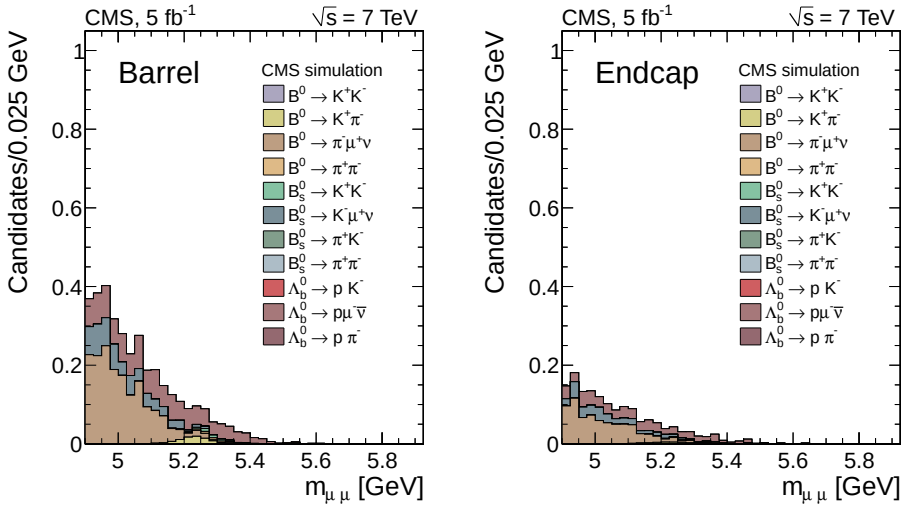

Figure 4: Simulated background from B decay in the barrel (left) and endcap (right) channels, normalized to the number of observed $B^+ \to J/\psi K^+ \to \mu^+\mu^- K^+$ events.

different acceptance, mainly because of different isolation. The acceptance ratio between signal and normalization is computed with simulation for the three production mechanisms and the biggest difference is taken as systematic error.

The uncertainty on the ratio of B^+ and $B^0_{d,s}$ production rates f_u/f_s is taken from LHCb measurement [9].

The uncertainties on the background coming from misidentified B hadron decays is estimated from the B production and branching ratio uncertainties, including the error on the misidentification probability.

Several experimental sources of systematic errors are considered: the uncertainties on trigger and muon identification efficiencies, selection efficiency, normalization events number and combinatorial background uncertainty. Other sources are specific for the normalization sample (K tracking efficiency) or the signal sample (mass resolution).

The uncertainties on trigger and muon identification efficiencies are estimated as the sum of two components; the first is taken as the variation of the efficiency when varying the p_T cuts, the other one is given by the difference of the efficiency in data and simulation using the tag-and-probe technique. The selection efficiency uncertainty is estimated by summing the differences in the efficiency for data and simulation for all the cuts.

The uncertainty on normalization events number is estimated by changing the fitting functions for signal and background. The combinatorial background uncertainty is estimated by varying the flight-length significance selections and by using a linear background shape with a variable slope.

The mass resolution effects, leading to migration of B^0_d decays to the B^0_s mass region and vice-versa, are estimated by comparing the J/ψ and $\Upsilon(1S)$ mass distributions in data and simulation. The muon tracking efficiency cancels in the signal/normalization ratio; the hadron tracking efficiency [12] affects the normalization sample.

As a crosscheck for the entire analysis chain the branching ratio $\mathfrak{B}(B^0_s \to J/\psi\phi \to \mu^+\mu^- K^+ K^-)$

source	barrel(%)	endcap(%)
Acceptance	3.5	5.0
f_s/f_u	8.0	8.0
B background	20.0	20.0
Data-MC efficiency (signal)	3.0	3.0
Data-MC efficiency (normalization)	4.0	4.0
K tracking efficiency (normalization)	4.0	4.0
Trigger efficiency	3.0	6.0
Muon id. efficiency	4.0	4.0
Normalization fit	5.0	5.0
Mass resolution	3.0	3.0
Combinatorial background	4.0	4.0

Figure 5: Summary of systematic uncertainties.

is evaluated using eq.2.1; this allows to check the correct calculation of the efficiencies and acceptances, the robustness of vertexing with a different number of final state particles and the absence of biases introduced by the selection. The result is in agreement with the world average [11]; moreover, the results for the barrel and endcap channels agree within the statistical uncertainties, showing the validity of extending the f_s/f_u measurement from LHCb to the barrel region. No systematic error is added following this crosscheck.

4. Results

The expected number of events from signal and background can be compared with the observed one; the signal mass window is splitted in two parts, 5.20 GeV $< M_{\mu^+\mu^-} <$ 5.30 GeV and 5.30 GeV $< M_{\mu^+\mu^-} <$ 5.45 GeV for B^0_d and B^0_s decays respectively. The summary of excpected and observed event numbers is shown in table 2 and the observed events mass distribution is shown in fig.6.

	$B^0_d \to \mu^+\mu^-$ 5.20 GeV $< m_{\mu^+\mu^-} <$ 5.30 GeV		$B^0_s \to \mu^+\mu^-$ 5.30 GeV $< m_{\mu^+\mu^-} <$ 5.45 GeV	
	Barrel	Endcap	Barrel	Endcap
Signal	0.24 ± 0.02	0.10 ± 0.01	2.70 ± 0.41	1.23 ± 0.18
B background	0.33 ± 0.07	0.15 ± 0.03	0.18 ± 0.06	0.08 ± 0.02
Combinatorial background	0.40 ± 0.34	0.76 ± 0.35	0.59 ± 0.50	1.14 ± 0.53
Sum	0.97 ± 0.35	1.01 ± 0.35	3.47 ± 0.65	2.45 ± 0.56
Observed	2	0	2	4

Table 2: Expected number of events for signal (SM-prediction) and background (peaking and combinatorial). The quoted errors include both, the statistical and the systematic uncertainties.

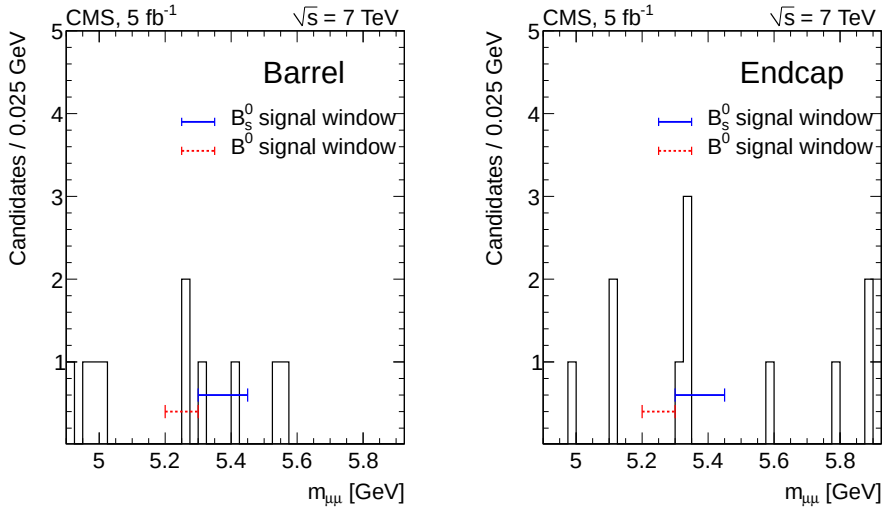

Figure 6: Dimuon invariant mass distribution in the barrel (left) and the endcap channel (right).

The observed numbers of events are consistent with the SM expectation for signal plus background and do not correspond to any excess, so a limit can be computed. Upper limits on $\mathfrak{B}(B_d^0 \to \mu^+\mu^-)$ and $\mathfrak{B}(B_s^0 \to \mu^+\mu^-)$ are computed by using the standard CL_s technique [13, 14]; the combined upper limits for the barrel and endcap channels are $\mathfrak{B}(B_s^0 \to \mu^+\mu^-) < 7.7 \times 10^{-9}$ and $\mathfrak{B}(B_d^0 \to \mu^+\mu^-) < 1.8 \times 10^{-9}$ at 95% confidence level. The corresponding median expected upper limits, based on the SM prediction, are 8.4×10^{-9} and 1.6×10^{-9} for $B_s^0 \to \mu^+\mu^-$ and $B_d^0 \to \mu^+\mu^-$ respectively; the p values are shown in table 3.

	95% CL limit	P-value (BG only)	P-value (BG + SM signal)
$B_d^0 \to \mu^+\mu^-$	1.8×10^{-9}	0.24	0.86
$B_s^0 \to \mu^+\mu^-$	7.7×10^{-9}	0.11	0.71

Table 3: Upper limits on $\mathfrak{B}(B_d^0 \to \mu^+\mu^-)$ and $\mathfrak{B}(B_s^0 \to \mu^+\mu^-)$ at 95% confidence level and p values. BG-only p-values assume freely-floating cross-feed, with each decay acting as a background for the other one.

5. Conclusions

A search for $B_s^0 \to \mu^+\mu^-$ and $B_d^0 \to \mu^+\mu^-$ decays to has been performed by CMS by analyzing proton-proton collisions at a center of mass energy $\sqrt{s} = 7$ TeV collected in 2011 corresponding to an integrated luminosity $\mathscr{L} = 5$ fb^{-1}. No excess was observed and a 95% confidence level upper limit has been set: $\mathfrak{B}(B_s^0 \to \mu^+\mu^-) < 7.7 \times 10^{-9}$ and $\mathfrak{B}(B_d^0 \to \mu^+\mu^-) < 1.8 \times 10^{-9}$.

References

[1] A. J. Buras, *Minimal flavour violation and beyond: Towards a flavour code for short distance dynamics*, *Acta Phys. Polon. B* **41** (2010) 2487 [1012.1447].

[2] J. R. Ellis, K. A. Olive, Y. Santoso et al., *On $B_s^0 \to \mu^+\mu^-$ and cold dark matter scattering in the MSSM with non-universal Higgs masses*, *JHEP* **05** (2006) 063 [hep-ph/0603136, doi:10.1088/1126-6708/2006/05/063].

[3] S. Davidson and S. Descotes-Genon, *Minimal flavour violation for leptoquarks*, *JHEP* **11** (2010) 073, [1009.1998, doi:10.1007/JHEP11(2010)073].

[4] S. R. Choudhury, A. S. Cornell, N. Gaur et al. *Signatures of new physics in dileptonic B-decays*, *Int. J. Mod. Phys. A* **21** (2006) 2617 [hep-ph/0504193, doi:10.1142/S0217751X06029491].

[5] J. Parry *Lepton flavor violating Higgs boson decays, $\tau \to \mu\gamma$ and $B_s^0 \to \mu^+\mu^-$ in the constrained MSSM+NR with large* $\tan\beta$, *Nucl. Phys. B* **760** (2007) 38 [hep-ph/0510305, doi:10.1016/j.nuclphysb.2006.10.011].

[6] J. R. Ellis, J. S. Lee, and A. Pilaftsis *B-Meson observables in the maximally CP-Violating MSSM with minimal flavour violation*, *Phys. Rev. D* **76** (2007) 115011 [0708.2079, doi:10.1103/PhysRevD.76.115011].

[7] C. Bobeth et al., *Enhancement of $\mathfrak{B}(B_d^0 \to \mu^+\mu^-)/\mathfrak{B}(B_s^0 \to \mu^+\mu^-)$ in the MSSM with minimal flavor violation and large* $\tan\beta$, *Phys. Rev. D* **66** (2002) 074021 [hep-ph/0204225, doi:10.1103/PhysRevD.66.074021].

[8] CMS Collaboration, *The CMS experiment at the CERN LHC*, *JINST* **03** (2008) S08004 [doi:10.1088/1748-0221/3/08/S08004].

[9] LHCb Collaboration, *Measurement of b hadron production fractions in* 7 TeV *pp collisions*, *Phys. Rev. D* **85** (2012) 032008 [1111.2357v2, doi:10.1103/PhysRevD.85.032008].

[10] CMS Collaboration *Performance of muon identification in pp collisions at $\sqrt{s} = 7$* TeV, *CMS Physics Analysis Summary* CMS PAS MUO-10-002 (2010).

[11] Particle Data Group, *Review of particle physics*, *J. Phys.* **37** (2010) 075021 [doi:10.1088/0954-3899/37/7A/075021].

[12] CMS Collaboration, *Measurement of Tracking Efficiency*, *CMS Physics Analysis Summary* CMS PAS TRK-10-002 (2010).

[13] T. Junk, *Confidence level computation for combining searches with small statistics*, *Nucl. Instrum. Meth. A* **434** (1999) 435 [hep-ex/9902006, doi:10.1016/S0168-9002(99)00498-2].

[14] A. L. Read, *Presentation of search results: The CL_s technique*, *J. Phys.* **28** (2002) 2693 [doi:10.1088/0954-3899/28/10/313].